JOURNAL OF GUIDANCE, CONTROL, AND DYNAMICS
Vol. 25, No. 4, July–August 2002

Relative Satellite Motion About an Oblate Planet

William E. Wiesel*
Air Force Institute of Technology, Wright–Patterson Air Force Base, Ohio 45433

A solution to the relative motion problem for satellites is constructed that is based on nearly circular reference periodic orbits and Floquet theory for the relative motion. This solution conceptually resembles the Clohessy–Wiltshire solution for relative motion, but includes all zonal harmonics of the Earth's gravitational field. Accuracy of this solution is at least three orders of magnitude better than the Clohessy–Wiltshire solution. We treat the effect of second-order displacements from the periodic solution via a semi-analytic perturbation theory. The effects of sectoral and tesseral gravity terms, as well as air drag, make their appearance as a particular solution to the linear Floquet problem. Comparisons are made between numerical integrations in the inertial frame and predictions from the periodic orbit/Floquet/modal perturbation theory, including all gravitational harmonics through order 14, as well as air drag. Submeter–10-m accuracy is achieved for representative clusters in a 1.1 Earth radii, one radian inclination orbit, over one half-day.

Introduction

RELATIVE motion of satellites is usually discussed following Clohessy and Wiltshire[1] (CW), who linearized the two-body problem of orbital mechanics about a circular orbit and solved the resulting constant coefficient linear system. Their solution will be familiar to most workers in the field of astronautics and is commonly used for planning and executing rendezvous and docking maneuvers. Recently, their work has been the underlying solution in many discussions of satellite cluster dynamics and control. However, rendezvous operations and satellite cluster dynamics have one very fundamental difference. In the rendezvous problem, one spacecraft executes a series of maneuvers over a very few orbits to bring about a docking. This is, relatively speaking, a problem where large maneuvers are expected, and the entire rendezvous and docking problem is over in only a day or so.

Satellite clusters, on the other hand, must fly in close proximity for years, and because the individual satellites may be small, it will not be possible to expend maneuvering fuel as prolifically as one does in the rendezvous problem. Any modeling deficiency in the dynamics will lead to unexpected satellite relative motion, and any inaccuracy in the prediction of that motion will lead to erroneous maneuvering to zero out possibly benign perturbations. It is noteworthy, in this regard, that, whereas the CW solution[1] has only one secular term (e.g., a term proportional to time t), Schaub and Alfriend[2] have shown that the relative motion problem with the Earth's oblateness J_2 included has two directions where solutions separate proportional to time.

Perturbations for cluster relative motion have been examined by a number of authors, virtually always in the context of the CW solution as the reference orbit. Sedwick et al.[3] examined perturbations from CW motion in an order of magnitude analysis. Melton[4] has expanded the state transition matrix for the two-body problem in a series in the eccentricity, whereas Carter[5] has produced an excellent survey of relative motion work, as well as a closed-form solution for the state transition matrix for the two-body problem. Gim and Alfriend[6] have produced the state transition matrix for the two-body problem perturbed by J_2. Much control work has been published, too numerous to cite here. Ulybyshev[7] used a time-averaged secular term form of the CW equations to study the effects of air drag. De Queiroz et al.[8] implemented a nonlinear controller, again based on the CW reference dynamics. Sparks[9] studied the effect of J_2 perturbations on a system with a linear quadratic regulator controller.

However, the method presented here differs fundamentally from the control problem approach. The author feels strongly that control should only be used as a last resort and only when perturbations act to disperse the cluster. The first step, then, is to produce a linearized reference solution that includes as much of the dynamics as possible, and the second step is to characterize all of the natural perturbations to the linear motion.

In this paper, the problem of satellite relative motion will be completely reexamined. By the use of a nearly circular periodic orbit as the reference solution, and by the use of Floquet theory[10] to solve the linear system, it is possible to produce a first-order relative motion solution that includes all zonal harmonics of the Earth's gravitational field. This solution may be expressed in several reference frames, including the familiar radial/orbit normal/in-track reference frame (the Hill frame) of the CW solution. The new solution also offers the advantage of the familiar expression

$$\delta\dot{\boldsymbol{x}} = A(t)\delta\boldsymbol{x} + B(t)\boldsymbol{u} \tag{1}$$

for the local dynamics control work, as well as the option to work in the same orbital reference frame made familiar by the CW solution. The effects of forces not included in the linear reference solution are traced carefully throughout the development. Perturbations to the linear system are studied, including quadratic and higher-order terms arising from the two-body and zonal harmonics model, air drag, and contributions from other gravitational harmonics.

This paper covers three basic topics. The first three sections discuss the existence and construction of periodic orbits in the zonal potential problem. This establishes the reference orbit for relative motion work. The next two sections discuss the construction of the solution to the linear time-periodic problem. These sections are the equivalent of the CW solution but incorporate much more of the full dynamics. Care is taken in these early sections to track how extra perturbing forces will appear in the problem as coordinate transformations are made. Finally, the last sections detail a full numerical/semi-analytic perturbation theory to include all other forces that appear in the motion of Earth satellites. The result is a complete theory of satellite relative motion in the vicinity of nearly circular orbits, to which control theory via Eq. (1) can be applied and in which the effects of perturbing forces have already been characterized.

Existence of Periodic Orbits

This paper reports the construction of periodic orbits about Earth in a dynamics model that includes the Newtonian point mass potential and (potentially) all of the zonal harmonics of the gravity field. This dynamic system is time invariant, and so the Hamiltonian is an integral of the motion, and because it is also invariant to rotations

Received 26 June 2000; revision received 26 October 2001; accepted for publication 8 February 2002.

*Professor, Astronautical Engineering, ENY. Member AIAA.

about the Earth's polar axis, the z component of angular momentum is also constant. This model, of course, includes the very important J_2 zonal harmonic. However, it is sometimes claimed that orbital motion about the Earth possesses no periodic orbits. The claim that they exist needs to be justified.

At the lowest level, imagine an exactly circular orbit subject to the classic secular perturbations due to J_2. The node will regress and, in a reference frame that moves with the ascending node (which we will call the nodal frame), the circular orbit will close on itself. Because the orbit is assumed exactly circular, the perigee will advance, but this makes no difference to a circular orbit. Only the orbital period, which is now the period from nodal crossing to nodal crossing, will be changed by the advance of the perigee.

Actually, the claim that the argument of perigee must always advance is not true for very small eccentricities. The classical secular perturbation theory that leads to this claim begins by ignoring all periodic terms in the disturbing function. These are at least of order one in the eccentricity, and if the eccentricity is very small they should be negligible. The secular part of the disturbing function yields the secular rates, and the effect of the small periodic terms can then be studied. However, the Lagrange planetary equation for the argument of perigee,

$$\frac{\mathrm{d}\omega}{\mathrm{d}t} = \frac{\sqrt{1-e^2}}{na^2e}\frac{\partial R}{\partial e} - \frac{\cot i}{na^2\sqrt{1-e^2}}\frac{\partial R}{\partial i} \tag{2}$$

in terms of the disturbing function R, is obviously singular for small eccentricity. Allegedly negligible periodic terms in the disturbing function that are of order eccentricity e in the disturbing function are of order $1/e$ in $\mathrm{d}\omega/\mathrm{d}t$. In other words, they are not negligible at all. The claim that the argument of perigee must always advance is unfounded for nearly circular orbits.

At a much higher level of approximation, there is a considerable literature on frozen orbits, including many successful applications to actual missions. The theory of frozen orbits treats the behavior of nearly circular orbits under the influence of secular perturbations from all of the zonal harmonics. (Note that we also will isolate all of the zonal harmonics.) Among many worthwhile efforts, we note Nickerson et al.[11] for an early discussion, whereas Rosborough and Ocampo[12] contains a more through treatment, and Shapiro[13] discusses flight experience with Topex/Poseidon, and his work contains a thorough bibliography. By the imposition of the constraint that the secular rate of the argument of perigee be zero, the theory of frozen orbits produces a very nearly circular orbit that remains nearly frozen in its apsidial orientation, while the orbit plane still regresses. These orbits exist for eccentricities so small that the separation of secular and periodic terms is clearly invalid. We will see shortly that the current paper essentially extends frozen orbit theory by including the periodic terms in the disturbing function, producing a true periodic orbit for the Newtonian plus zonal harmonics gravity problem.

Reference Periodic Orbit

Begin in the usual Earth-centered inertial frame, with rectangular coordinates X, Y, and Z, with Z along the Earth's polar axis. We will use dimensionless units with the radius of the Earth $R_\oplus = 1$, the gravitational constant $G = 1$, and the mass of the Earth $M_\oplus = 1$. The problem of orbital motion about the Earth, restricted to the zonal harmonics, has the Hamiltonian function

$$\mathcal{H} = \frac{1}{2}\left\{P_X^2 + P_Y^2 + P_Z^2\right\} - \frac{1}{r} + \frac{1}{r}\sum_{i=2}^{\infty}\left(\frac{1}{r}\right)^i J_i P_i^0\left(\frac{Z}{r}\right) \tag{3}$$

where, of course, $r = \sqrt{(X^2 + Y^2 + Z^2)}$, the zonal gravity coefficients $C_{i0} = -J_i$, and $P_i^0(Z/r)$ is the Legendre polynomial of order i. The dynamic system (3) possesses time-reversal symmetry and is symmetric about the Z axis. Hence, both the total energy $\mathcal{H}$ and the Z component of angular momentum

$$L_Z = XP_Y - YP_X \tag{4}$$

are conserved. The momenta P_i are just the inertial velocity components because Eq. (3) is a Hamiltonian per unit mass of satellite. As a convenient shorthand, we will write the inertial frame state vector as $\mathcal{I}^T = (X, Y, Z, P_X, P_Y, P_Z)$. Note that, whereas the sum over the zonal harmonics will in practice be truncated at some finite limit, in theory all of the zonal harmonics can be included in the periodic orbit and relative motion solution.

Nearly circular periodic orbits exist in this system at any inclination and orbital radius but only in a reference frame regressing about the Z axis at the (as yet unknown) nodal regression rate. For definiteness, pick initial conditions at $t = 0$ on the X axis with a fixed initial inclination i_0 and fixed initial radius r_0 as

$$X = r_0, \qquad Y = 0, \qquad Z = 0, \qquad P_X = \dot{r}_0$$
$$P_Y = S_0\cos i_0, \qquad P_Z = S_0 \sin i_0 \tag{5}$$

where the period τ, the radial velocity $\dot{r}_0$, and the tangential speed S_0 are initial parameters to be determined from the solution of a periodic orbit boundary-value problem. These three unknown initial conditions are to be determined by enforcing the final boundary conditions at one period, $t = \tau$:

$$Z(\tau) = 0, \qquad r(\tau) = r_0, \qquad \boldsymbol{r}(\tau)\cdot\boldsymbol{P}(\tau) = r_0\dot{r}_0 \tag{6}$$

These conditions state that the satellite must again be crossing the plane $Z = 0$ at τ, that it be at the same distance from the Earth r_0, and that it have the same radial velocity $\dot{r}_0$. The radial velocity component $\dot{r}_0$ is necessary because the odd-order zonal harmonics, for example, J_3, introduce a north/south asymmetry into the problem. The particular form of the final conditions (6) has been chosen to be independent of the (still unknown) nodal regression rate. Conservation of energy and the Z component of angular momentum then suffice to force both the initial tangential speed S_0 and the initial inclination i_0 to return to their initial values. We have implemented this algorithm numerically. Typically, we have observed that all six initial and final conditions match to at least 10 and usually 12 significant figures, when compared in the rotating frame of reference.

The orbit does not return to the same position in inertial space. The point at which the orbit closes on itself will have regressed along the equator, and so the orbit is only truly periodic in a rotating frame of reference. Once the periodic orbit has been found, we can calculate the amount of rotation of the initial position about the Z axis $\cos\theta = \boldsymbol{r}(0)\cdot\boldsymbol{r}(\tau)/r_0^2$. Then, define an average regression rate for the node as

$$\dot{\Omega} = -\theta/\tau \tag{7}$$

and write a rotation matrix about the Z axis as

$$\mathcal{R}_Z = \begin{Bmatrix} \cos(\Omega_0 + \dot{\Omega}t) & \sin(\Omega_0 + \dot{\Omega}t) & 0 \\ -\sin(\Omega_0 + \dot{\Omega}t) & \cos(\Omega_0 + \dot{\Omega}t) & 0 \\ 0 & 0 & 1 \end{Bmatrix} \tag{8}$$

Including the initial right ascension of the node Ω_0 removes any special orientation for the periodic orbit. Then, the rotation transformation

$$(X', Y', Z')^T = \mathcal{R}_Z(X, Y, Z)^T$$
$$(P_X', P_Y', P_Z')^T = \mathcal{R}_Z(P_X, P_Y, P_Z)^T \tag{9}$$

is canonical, with a new Hamiltonian

$$\mathcal{H}' = \tfrac{1}{2}\left\{P_X'^2 + P_Y'^2 + P_Z'^2\right\} + \dot{\Omega}(P_X'Y' - P_Y'X') + V(Z', r) \tag{10}$$

It is in this coordinate frame that the periodic orbit actually closes on itself. We will refer to this reference frame as the nodal frame.

The noninertial effects of the rotating frame are accounted for by the cross product term $P_X'Y' - P_Y'X'$ in the Hamiltonian (10). The transformation (9) shows that the new momenta P_i' are still the inertial velocity components, now expressed in their components in the rotating nodal frame. This means that nonconservative forces are simply added in the momenta equations of motion, and we need only resolve them in the nodal frame to include their effects. Of course, conservative perturbing forces are included by adding a potential term to the Hamiltonian itself.

These periodic orbits exist for any value of the orbital radius and inclination. Figure 1 shows the difference between the two-body circular orbit values of speed V_{circ}, Keplerian period T_k, and radial velocity (zero), for the periodic orbit speed S_0, period τ, and radial velocity $\dot{r}_0$ at an inclination of $i_0 = 0.5$ rad. These differences are all of order J_2, indicating that we are looking at small, oblateness engendered effects.

The coordinates of the periodic orbit in the nodal reference frame close on themselves and can be conveniently reduced to Fourier series.[14] By examination of the Fourier coefficients, it is very easy to truncate the summation at a level that guarantees a desired accuracy, and, of course, the series representation can be numerically compared to the periodic orbit to confirm this. We have found that retaining the first 30 terms approaches full double-precision accuracy. When the canonical state vector is written in the nodal frame as $\mathcal{N}^T = (X', Y', Z', P'_X, P'_Y, P'_Z)$, the inertial and nodal states are related by $\mathcal{N} = \mathcal{R}_Z^{(2)} I$, where $\mathcal{R}_Z^{(2)}$ is a six by six block diagonal matrix with two copies of $\mathcal{R}_Z$ on the diagonal. We will write $\mathcal{N}_0(t)$ as a shorthand for the periodic orbit itself.

We return to the relationship between the periodic orbits of the current paper and frozen orbit theory. Figure 2 shows the variation of the osculating elements $e\cos\omega$, $e\sin\omega$ over one cycle of the periodic orbit, for the case of an initial radius of 1.1 Earth radii and an inclination of 1 rad. Also plotted as a point are the approximate values of these quantities in frozen orbit theory, extracted from the plots by Rosborough and Ocampo.[12] These were computed for a gravity field including zonal terms through order 50, whereas we have only used terms through order 14. The author feels that the agreement is quite satisfactory, given the difference in gravity models and that we are describing slightly different objects. Frozen orbit theory does not include the periodic part of the zonal disturbing potential, whereas periodic orbit theory includes all of the zonal disturbing potential. The osculating orbital elements show that the argument of perigee ω is librating about $\omega = 90$ deg, as is expected in frozen orbit theory. In fact, it cycles four times per orbit. Apparently, the current theory of periodic orbits in a zonal potential is a somewhat more complete version of frozen orbit theory, which treats only the secular terms in the potential.

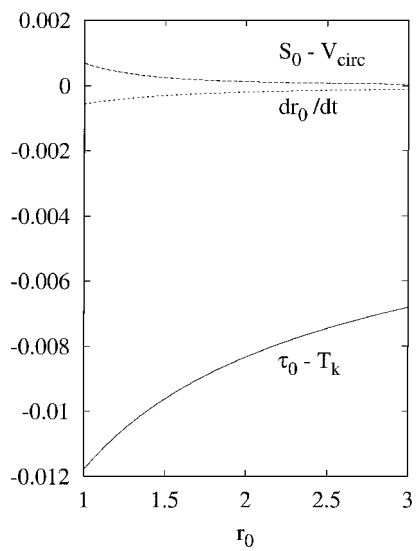

Fig. 1 Differences between the periodic orbit initial conditions and their Keplerian values.

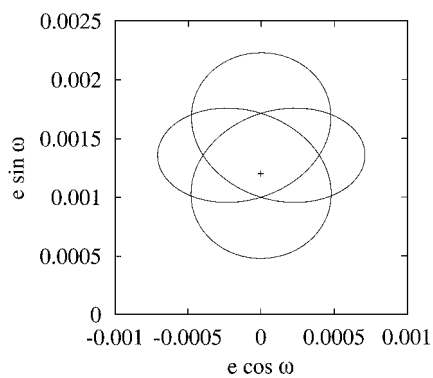

Fig. 2 Periodic orbit for one revolution plotted on the osculating $e\cos\omega$, $e\sin\omega$ plane.

Orbital Reference Frame

The reference orbit is periodic in a frame that regresses with the plane of the orbit. However, that is not the only frame in which the orbit is periodic. Our goal is to produce a solution that resembles the CW solution but includes much more of the total dynamics. Also, it is desirable to be able to handle further perturbing forces, for example, sectoral and tesseral harmonics, as well as nonconservative forces such as air drag.

Introduce coordinates relative to the periodic orbit:

$$\begin{aligned} x &= X' - X'_0(t), & p_x &= P'_X - P'_{X0}(t) \\ y &= Y' - Y'_0(t), & p_y &= P'_Y - P'_{Y0}(t) \\ z &= Z' - Z'_0(t), & p_z &= P'_Z - P'_{Z0}(t) \end{aligned} \tag{11}$$

where the quantities subscripted with zero refer to the periodic orbit. This transforms the periodic orbit to the origin of the coordinates. As shown by Wiesel,[15] this is canonical and reduces the Hamiltonian function to its quadratic and higher-order parts, evaluated on the periodic orbit. That is, if we assemble the local coordinates and momenta into a state vector $\mathcal{Y}^T = (x, y, z, p_x, p_y, p_z)$, the new Hamiltonian is

$$\mathcal{H}'' = \tfrac{1}{2!}\mathcal{H}''_{\alpha\beta}\mathcal{Y}_\alpha\mathcal{Y}_\beta + \tfrac{1}{3!}\mathcal{H}''_{\alpha\beta\gamma}\mathcal{Y}_\alpha\mathcal{Y}_\beta\mathcal{Y}_\gamma + \cdots \tag{12}$$

where repeated Greek indices are summed from one to six and Roman indices (when they occur) can freely take on values from one to six. Here, each $\mathcal{H}''_{\alpha\beta\ldots}$ is a fully symmetric partial derivative tensor evaluated on the periodic orbit:

$$\mathcal{H}''_{\alpha\beta} = \left.\frac{\partial^2\mathcal{H}'}{\partial\mathcal{N}_\alpha\partial\mathcal{N}_\beta}\right|_{\mathcal{N}_0(t)} \tag{13}$$

$$\mathcal{H}''_{\alpha\beta\gamma} = \left.\frac{\partial^3\mathcal{H}'}{\partial\mathcal{N}_\alpha\partial\mathcal{N}_\beta\partial\mathcal{N}_\gamma}\right|_{\mathcal{N}_0(t)} \tag{14}$$

For perturbation and control work, it is necessary to track how to reintroduce any dynamic effects that have been neglected. Forces that we have not yet included in the problem are handled in a very straightforward way. Conservative forces have a potential energy function, and this is expanded about the periodic orbit due to the change of origin (11). The zeroth-order (in $\mathcal{Y}$) terms perturb the periodic orbit itself, and linear and higher terms in $\mathcal{Y}$ perturb the relative motion. Nonpotential forces such as air drag are also expanded about the periodic orbit, and because the p_i are still inertial velocity components, their effects appear only in Hamilton's equations for the momenta states. As with conservative forces, only the linear and higher terms in these forces perturb the relative motion.

Now, introduce another set of coordinates that are the standard reference frame used in the CW solution. Define unit vectors tied to the reference periodic orbit, where the first vector is radial, $\boldsymbol{u}_1 = \boldsymbol{r}/r$, where $\boldsymbol{r}$ is the nodal frame position vector, the third vector is the orbit normal, $\boldsymbol{u}_3 = (\boldsymbol{r}\times\boldsymbol{v})/|\boldsymbol{r}\times\boldsymbol{v}|$, where $\boldsymbol{v}$ is the nodal frame velocity vector, and the second vector, $\boldsymbol{u}_2 = \boldsymbol{u}_3 \times \boldsymbol{u}_1$, lies near the velocity vector. Assembling these orthogonal unit vectors into a rotation matrix

$$\mathcal{R}^T = \{\boldsymbol{u}_1 \quad \boldsymbol{u}_2 \quad \boldsymbol{u}_3\} \tag{15}$$

we can introduce new coordinates in the radial, in-track, and orbit normal directions as

$$\begin{pmatrix} q_r \\ q_v \\ q_n \end{pmatrix} = \mathcal{R} \begin{pmatrix} x \\ y \\ z \end{pmatrix} \tag{16}$$

Again, this rotation generates a canonical transformation. The generating function is just

$$F_2 = \begin{pmatrix} p_r \\ p_v \\ p_n \end{pmatrix} \cdot \mathcal{R} \begin{pmatrix} x \\ y \\ z \end{pmatrix} \tag{17}$$

and the momenta transform as $(p_r, p_v, p_n)^T = \mathcal{R}(p_x, p_y, p_z)^T$. Write the new canonical state vector as $\mathcal{Z}^T = (q_r, q_v, q_n, p_r, p_v, p_n)$. It is this set of coordinates that mimic the usual radial/in-track/orbit normal coordinates of the CW solution. (We note here that satellites may use the horizon and orbit normal for their reference frame, rather than the actual radius vector. There is a slight difference due to the nonspherical shape of the Earth. This rotation transformation could just as easily use the horizon from an ellipsoidal Earth model for the reference direction, and the discussion to follow will be unchanged, although slightly different results will be obtained numerically. The matrix $\mathcal{R}$ need only be periodic to preserve the structure of the Floquet solution to follow.)

The quadratic part of the Hamiltonian (which, of course, generates a linear dynamic system) transforms into the variables $\mathcal{Z}$ as

$$\mathcal{K}_2 = \frac{1}{2}\mathcal{H}''_{\alpha\beta}\mathcal{Y}_\alpha\mathcal{Y}_\beta + \frac{\partial F_2}{\partial t} = \frac{1}{2}\mathcal{H}''_{\alpha\beta}\mathcal{R}^{(2)}_{\alpha\gamma}\mathcal{R}^{(2)}_{\beta\delta}\mathcal{Z}_\gamma\mathcal{Z}_\delta + \boldsymbol{p}\cdot\dot{\mathcal{R}}\mathcal{R}^T\boldsymbol{q} \tag{18}$$

The matrix $\mathcal{R}^{(2)}$ is just the orbital frame rotation matrix repeated twice:

$$\mathcal{R}^{(2)} = \begin{Bmatrix} \mathcal{R} & 0 \\ 0 & \mathcal{R} \end{Bmatrix} \tag{19}$$

and the second term in Eq. (18) is the cross product to be expected when transforming to a rotating frame of reference. Higher-order terms in the Hamiltonian transform more directly, for example, the third-order contributions to the Hamiltonian (18) are

$$\tfrac{1}{3!}\mathcal{K}_{\alpha\beta\gamma}\mathcal{Z}_\alpha\mathcal{Z}_\beta\mathcal{Z}_\gamma = \tfrac{1}{3!}\mathcal{H}''_{\lambda\sigma\tau}\mathcal{R}^{(2)}_{\lambda\alpha}\mathcal{R}^{(2)}_{\sigma\beta}\mathcal{R}^{(2)}_{\tau\gamma}\mathcal{Z}_\alpha\mathcal{Z}_\beta\mathcal{Z}_\gamma \tag{20}$$

and so forth. Again, the momenta states p_r, p_v, and p_n are still the inertial velocity components relative to the periodic orbit, but now expressed in the unit vectors of the orbital frame. This means that nonpotential forces are simply expanded about the periodic orbit and then added to Hamilton's equations of motion for the momenta states once they have been resolved in the orbital reference frame.

Floquet Solution

The relative motion solution we are seeking is, like the CW treatment, a solution to a linear system. However, expanding about the periodic orbit, the linearized equations derived from Eq. (18) are periodic in time. The solution to such problems was first found by Floquet[10] and has been discussed by many authors since.

The relative motion Hamiltonian (18), restricted to its quadratic part, generates the matrix linear system

$$\dot{\Phi} = A\Phi, \qquad \Phi(t=0) = I \tag{21}$$

where the plant matrix A comes directly from Hamilton's equations of motion. Integrating this matrix differential equation for one orbit gives the monodromy matrix $\Phi(\tau, 0)$. Now, according to Floquet, the state transition matrix Φ factors as

$$\Phi(t, 0) = F(t)e^{\mathcal{J}t}F^{-1}(0) \tag{22}$$

The periodic modal matrix $F(t)$ and the Jordan form of Poincaré exponents $\mathcal{J}$ must be constructed to find this solution. The initial matrix $F(0)$ is just the eigenvector matrix of $\Phi(\tau, 0)$, as evaluating Eq. (22) at $t = \tau$ will show. The eigenvalues of the monodromy matrix μ_i, termed the characteristic multipliers, are related to the Poincaré exponents $\mathcal{J}_{ii}$ by $\mathcal{J}_{ii} = \log\mu_i/\tau$. Substituting Eq. (22) into Eq. (21) and simplifying produces

$$\dot{F} = AF - F\mathcal{J} \tag{23}$$

This differential equation, propagated for one period, allows the periodic matrix $F(t)$ to be found and reduced numerically to Fourier series form.

However, the current problem is not quite this simple. Because we have two integrals of the motion, there are two pairs of zero Poincaré exponents, and each has an associated generalized eigenvector. General purpose eigenvalue/vector software is written assuming that the eigenvalues are distinct and will find only three of the six eigenvectors. However, the full set of eigenvectors associated with the four zero Poincaré exponents can be easily constructed from the system's fundamental symmetries, as will now be described. For definiteness, denote the nondegenerate modal vectors as $\boldsymbol{f}_1$ and $\boldsymbol{f}_2$, with purely imaginary Poincaré exponents. (We are using a numbering scheme that will keep canonically conjugate Floquet modes adjacent to each other in the problem.) The first eigenvector with a zero Poincaré exponent is just the periodic orbit phase space velocity vector, $\boldsymbol{f}_3 = \mathcal{R}\,\mathrm{d}\mathcal{N}_0/\mathrm{d}t$ in the orbital reference frame, suitably normalized. The second eigenvector with zero Poincaré exponent is due to symmetry of the problem about the Z axis and is in the direction of a rigid rotation of the initial conditions about that axis, again expressed in the orbital frame. That is,

$$\boldsymbol{f}_5 = \begin{pmatrix} \mathcal{R}\boldsymbol{k} \times \boldsymbol{r} \\ \mathcal{R}\boldsymbol{k} \times \boldsymbol{P}' \end{pmatrix} \tag{24}$$

where $\boldsymbol{k}$ is the Z axis unit vector. These are normal eigenvectors of $\Phi(\tau, 0)$. The remaining two eigenvectors are generalized eigenvectors and satisfy

$$(\Phi - I)\boldsymbol{f}_4 = \tau\boldsymbol{f}_3, \qquad (\Phi - I)\boldsymbol{f}_6 = \tau\boldsymbol{f}_5 \tag{25}$$

These equations will still be singular because $\Phi - I$ has four zero eigenvalues. Note that each generalized eigenvector is undetermined to within addition of an arbitrary multiple of the normal eigenvector: $\boldsymbol{f}'_4 = \boldsymbol{f}_4 + \gamma\boldsymbol{f}_3$. Substituting the conditions $\boldsymbol{f}_j \cdot \boldsymbol{f}_3 = 0$ and $\boldsymbol{f}_j \cdot \boldsymbol{f}_5 = 0$ for two rows of the preceding will resolve this ambiguity. Also note the extra factor of τ on the right compared to the usual definition of generalized eigenvectors. This factor is necessary to match the Jordan normal form for this type of orbit, which will have two nonzero diagonal elements and two blocks of the form

$$\begin{Bmatrix} 0 & 1 \\ 0 & 0 \end{Bmatrix} \tag{26}$$

These Jordan blocks give rise to two terms linear in time in the quantity $e^{\mathcal{J}t}$. In turn, this means that there are two directions in phase space where a satellite can drift away from the reference orbit, instead of the usual one direction familiar from the CW solution. The second linear drift direction was first described by Schaub and Alfriend.[2] More details on the construction of degenerate Floquet modal eigenvectors can be found in Refs. 15 and 16.

The modal matrix $F(t)$ can now be propagated for one orbit via Eq. (23) and conveniently reduced to Fourier series form. By the inclusion of the nodal regression rotation, the periodic orbit, and the first-order Floquet solution, the inertial position vector of a satellite can be written as

$$I(t) = R_Z^{(2)\,T}\left\{\mathcal{N}_0(t) + \left(\mathcal{R}^{(2)}\right)^T F(t)e^{\mathcal{J}t}F^{-1}(t_0)\mathcal{Z}(t_0)\right\} \tag{27}$$

whereas in the orbital frame, the position of the satellite relative to the periodic orbit is given by

$$\mathcal{Z}(t) = F(t)e^{\mathcal{J}t}F^{-1}(t_0)\mathcal{Z}(t_0) \tag{28}$$

This result includes potentially all zonal harmonics of the Earth's gravitational field and, like the CW equations, is correct to the first order in small displacements from the reference orbit. The expressions (27), for the inertial position, and Eq. (28), for the relative

spacecraft positions, are conceptually identical to their CW equivalents. However, the current solution includes all zonal harmonic perturbations through the first order in small displacements from the reference orbit, including the very important J_2 term. The solution itself consists of one periodic six-vector $\mathcal{N}_0(t)$, expressed as a Fourier series, one periodic six by six matrix $F(t)$, also reduced to Fourier series, the constant matrix $\mathcal{J}$, and the nodal regression rate $\dot{\Omega}$.

Floquet theory has many numerical checks that have been performed in this effort. We have already noted that initial and final conditions in the periodic orbit construction match to essentially double-precision accuracy. The degenerate eigenvectors (24) and (25) associated with this problem also generally satisfy the eigenvalue problem for Φ to double-precision accuracy. A strong check is that the numerical solution to Eq. (23) is actually periodic, as Floquet theory predicts. We usually achieve this condition to about 9–10 significant figures. Numerically, we observe a very strong decrease in the size of the Fourier coefficients with order, so that truncation becomes a simple matter. Usually about the first 30 Fourier coefficients contain all of the information in the full numerical integration. After reduction of the periodic orbit and modal matrix to truncated Fourier series, we have routinely compared the summed series version to another numerical integration with a different, incommensurable point spacing. This check matches the periodic orbit and modal matrix to well over 10 significant figures.

Linear Solution Behavior

In this section, we describe the Floquet[10] mode shapes of the solution. This will point out the similarities and differences with the more familiar CW solution. All results shown here are for a periodic orbit with an initial $r_0 = 1.1$ Earth radii (about 630-km altitude), and an inclination of 1 rad. We will also show results comparing the CW solution to the current method.

We begin with the one nondegenerate mode, which exists principally in the in-track/vertical direction. It has a nonzero pair of Poincaré exponents that take the form $\mathcal{J}_{11,22} = 0 \pm i\omega_1$, and the modal frequency ω_1 is of order J_2. Because the periodic modal vectors have a period of one orbit, and the modal frequency is of order J_2, we interpret this mode as the equivalent of the eccentricity mode in the CW solution. The equivalent motion in the CW solution is a simple ellipse in the radial/in-track plane, with a period of one orbit and a ratio of axis lengths of 2:1, and the current mode is very close to this. In the current solution, however, this mode also includes both the secular advance of the perigee and periodic perturbations in the eccentricity itself. The periodic modal vectors $\boldsymbol{f}_1(t)$ and $\boldsymbol{f}_2(t)$ (the first two columns of F) model the usual 2:1 ellipse (with some J_2 and higher perturbations), whereas the Poincaré exponent ω_1 is the expected secular motion of the perigee. Solution (28) has been used to construct Fig. 3, which shows the motion of this mode.

The remaining two Floquet modes are both degenerate and have one modal vector that does not engender a term linear in time in the solution and another that does. For the degenerate mode caused by the conservation of energy, the modal vector $\boldsymbol{f}_3$ is the periodic orbit velocity vector. A displacement along this vector will produce a nearly static time displacement between the reference periodic orbit and the satellite. The conjugate extended eigenvector $\boldsymbol{f}_4$ will produce a linear drift (secular term) in the in-track direction, with a nearly static displacement in altitude. This is a behavior that is conceptually the same as the CW solution, where the corresponding mode combines a change in orbital period with an in-track drift. The modal vector $\boldsymbol{f}_5$ appears as a nearly horizontal oscillation, although not through the origin of the coordinate frame. This mode is a slight change in the node of the nearby satellite relative to the reference periodic orbit. The conjugate extended eigenvector $\boldsymbol{f}_6$ models the effects of a slight change in inclination (and other elements), which would induce a relative precession of the orbit plane under J_2 perturbations, as found by Schaub and Alfriend.[2] The Floquet solution, thus, shows all of the behaviors familiar from the CW solution, as well as the expected J_2 effects on the relative motion.

We have also attempted accuracy comparisons between the CW solution and our results. The equations of motion resulting from Eq. (10) have been integrated numerically using a standard fourth-order predictor–corrector integrator that is strongly numerically stable . Initial conditions were chosen using Eq. (27), so that individual Floquet modes could be selectively studied. Of course, the CW results represent an exact solution within the linear regime for relative motion near a circular orbit in the two-body problem, just as our results are an exact solution within the linear regime for motion near a nearly circular periodic orbit in the zonal harmonics problem. Because the CW solution will be exercised out of its original setting, it will, of course, not do as well as the current method. However, the current dynamics model, especially including the first oblateness harmonic J_2, will be much closer to reality than is the two-body problem. We also have elected to give the CW solution every possible advantage and have only asked that it model the displacements from our precessing periodic orbit, rather than displacements from a nonrotating circular orbit. The CW solution was also given the correct orbital frequency from the periodic orbit. There is not an exact match between the dynamics of Eq. (10) and our solution either because higher-order nonlinear terms about the reference periodic orbit have been dropped in our method.

Figure 4 shows the results of this comparison for a period of one week, with only the eccentricity mode excited. The initial amplitude was approximately 500-m displacement from the reference orbit, which again was at 630-km altitude with an inclination of 1 rad. Note that the vertical axis, position error magnitude, is logarithmic, so that both solutions are departing roughly linearly in time from the results of the numerical integration. In the case of the Floquet solution, this could either be due to the influence of nonlinear terms that are present in the numerical integration and absent in the linear Floquet solution, or it could be numerical drift in the integration of Eq. (10). Subtraction of the periodic orbit reference state from the numerical integration produces a large amplification

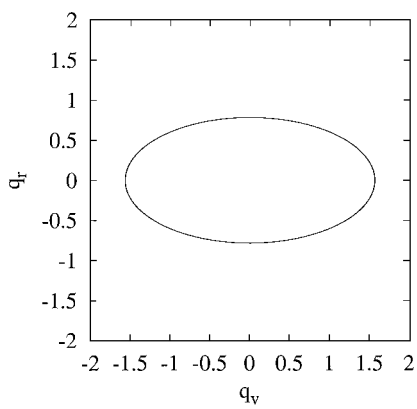

Fig. 3 Eccentricity mode lies mainly in the vertical/in-track direction.

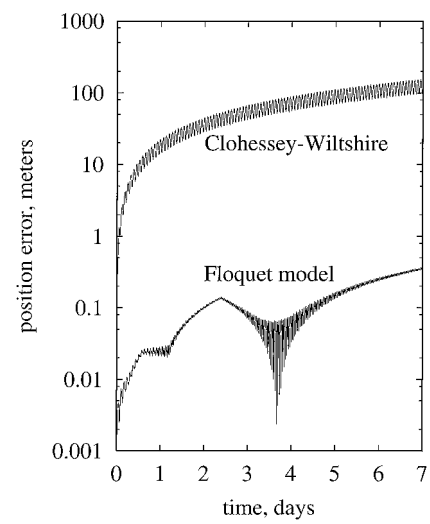

Fig. 4 Position error for the current (Floquet) solution and the CW solution.

of numerical errors, but the author feels very confident in the accuracy of the numerical integration and so interprets the discrepancy as the limitations of the first-order Floquet theory. The accuracy of the CW solution is uniformly two to three orders of magnitude worse, and within a week the position error reaches the same order of magnitude as the oscillation itself. This occurs in spite of the CW solution being given the correct orbital frequency and that it has been extended to include the nodal regression of the orbit plane. When used for rendezvous operations, note that the accuracy is fairly good for a day or so, which is usually more than the time interval used in final approach and docking. The improvement in the Floquet solution, around 3.7 days, the author believes to be an unusual situation, where the integration and the theory closely approach each other once per orbit. This, of course, can not be depended on to always happen.

Perturbation Theory

The development to here has been the analog of CW theory, with a periodic orbit in a zonal potential replacing the circular two-body orbit, and the linear Floquet solution replacing the constant coefficient linear system solution of CW. However, this is not yet a complete description of relative satellite motion.

The Floquet problem can be separated in either the nodal or orbital frame of reference. We will find it advantageous to return to the nodal frame Hamiltonian (12) because higher-order gravity harmonics are more easily expressed in the nodal reference frame. The equations of motion can be written (with nonconservative forces included) as

$$\frac{\mathrm{d}}{\mathrm{d}t}\mathcal{Y}_i = A_{i\alpha}(t)\mathcal{Y}_\alpha + \frac{1}{2!}B_{i\alpha\beta}(t)\mathcal{Y}_\alpha\mathcal{Y}_\beta + \cdots + \mathcal{R}_Z^{(2)}\begin{Bmatrix}0\\ \boldsymbol{a}_p(t)\end{Bmatrix} \qquad i = 1, 6 \quad (29)$$

where $\mathcal{R}_Z^{(2)}$ is the rotation matrix from the inertial to the nodal reference frame. Each tensor given is periodic and fully symmetric on every index after the first and can be written in terms of partial derivatives of the nodal frame Hamiltonian $\mathcal{H}'$:

$$A_{ij}(t) = Z_{i\alpha}\left.\frac{\partial^2\mathcal{H}'}{\partial\mathcal{N}_\alpha\partial\mathcal{N}_j}\right|_{\mathcal{N}_0(t)} \quad (30)$$

$$B_{ijk}(t) = Z_{i\alpha}\left.\frac{\partial^3\mathcal{H}'}{\partial\mathcal{N}_\alpha\partial\mathcal{N}_j\partial\mathcal{N}_k}\right|_{\mathcal{N}_0(t)} \quad (31)$$

and so forth. Here, Z is the usual symplectic matrix

$$Z = \begin{Bmatrix}0 & I\\ -I & 0\end{Bmatrix} \quad (32)$$

required to produce the sign structure of Hamilton's equations of motion. As periodic functions, these matrices can be calculated and reduced to Fourier series around the periodic orbit. The nodal frame Hamiltonian $\mathcal{H}'$ includes the two-body and zonal harmonics, so that all other effects are included in the perturbing acceleration $\boldsymbol{a}_p$. The quantities $\boldsymbol{a}_p(t)$ in Eq. (29) are any extra perturbing acceleration components on the system that were not included in the two-body/zonal harmonics baseline model. These are inertial acceleration components transformed to the nodal reference frame by the nodal regression rotation matrix $\mathcal{R}_Z^{(2)}$, and their lowest-order terms are those found by evaluation on the periodic orbit itself, with further expansion in $\mathcal{Y}$ components possible.

The Floquet solution makes it possible to separate variables and to introduce new coordinates ideally suited to perturbation theory. When the periodic modal matrix in the nodal frame are written as E, introduce the new variables z by

$$\mathcal{Y} = E(t)z = \mathcal{R}^{(2)}(t)F(t)z \quad (33)$$

that is, $\boldsymbol{F}(t)$ is the orbital reference frame periodic Floquet modal matrix used in earlier sections, $\mathcal{R}^{(2)}$ is the six by six orbital to nodal frame rotation matrix, and $E(t)$ is the nodal frame Floquet modal matrix. We will find the use of $E(t)$ more convenient for perturbation work because higher-order gravitational perturbations are more easily expressed in the nodal than in the orbital frame. The very important system state vector $z(t)$ is the set of six Floquet modal amplitudes. We have used the common transformation of isolating the real and imaginary parts of the one complex mode,[17] so that both $E(t)$ and $F(t)$ in Eq. (33) are purely real matrices. Then, substituting Eq. (33) into Eq. (29) and using the definition of the Floquet modal matrix gives

$$\frac{\mathrm{d}}{\mathrm{d}t}z = (E^{-1}AE - E^{-1}\dot{E})z = \mathcal{J}z \quad (34)$$

Here, $\mathcal{J}$ is the constant Jordan normal form for this type of periodic orbit:

$$\mathcal{J} = \begin{Bmatrix}0 & +\omega_1 & 0 & 0 & 0 & 0\\ -\omega_1 & 0 & 0 & 0 & 0 & 0\\ 0 & 0 & 0 & 1 & 0 & 0\\ 0 & 0 & 0 & 0 & 0 & 0\\ 0 & 0 & 0 & 0 & 0 & 1\\ 0 & 0 & 0 & 0 & 0 & 0\end{Bmatrix} \quad (35)$$

where the modal frequency ω_1 is now real. We will refer to the z as the modal variables and to individual modes as the eccentricity mode (rows and columns 1 and 2, the only mode with purely oscillatory behavior), the energy mode (rows and columns 3 and 4), and the angular momentum mode (rows/columns 5 and 6). Applying this transformation to the entire expansion (29) then produces

$$\frac{\mathrm{d}}{\mathrm{d}t}z_i = \mathcal{J}_{i\alpha}z_\alpha + \frac{1}{2!}E^{-1}_{i\alpha}B_{\alpha\beta\gamma}E_{\beta\delta}E_{\gamma\epsilon}z_\delta z_\epsilon + \cdots + E^{-1}\mathcal{R}_Z^{(2)}\begin{Bmatrix}\boldsymbol{0}\\ \boldsymbol{a}_p(t)\end{Bmatrix} \quad (36)$$

Again, the term with the perturbing accelerations is only the zeroth-order term in an expansion in z. These equations separate variables in the linear part of the system and are ideal for studying perturbations in the relative motion.

Second-Order Two-Body/Zonal Perturbations

The current solution includes the two-body problem, all zonal harmonics in both the periodic orbit and the Floquet solution, and the first order in small quantities with respect to the periodic orbit. One of the largest sources of perturbations then is likely to be the second- and higher-order terms in the variational equations, especially the two-body terms. In the modal variables, the first-order solution to Eq. (36) can be written as

$$z(t) = e^{\mathcal{J}(t-t_0)}z(t_0) \quad (37)$$

When $\delta t = t - t_0$ is abbreviated, the matrix $e^{\mathcal{J}\delta t}$ is easily found to be

$$e^{\mathcal{J}\delta t} = \begin{Bmatrix}\cos\omega_1\delta t & \sin\omega_1\delta t & 0 & 0 & 0 & 0\\ -\sin\omega_1\delta t & \cos\omega_1\delta t & 0 & 0 & 0 & 0\\ 0 & 0 & 1 & \delta t & 0 & 0\\ 0 & 0 & 0 & 1 & 0 & 0\\ 0 & 0 & 0 & 0 & 1 & \delta t\\ 0 & 0 & 0 & 0 & 0 & 1\end{Bmatrix} \quad (38)$$

Of course, the inverse of this matrix is just $e^{-\mathcal{J}\delta t}$.

We begin by assuming that the first-order solution (37) is sufficiently accurate to be used to evaluate the second-order perturbing term. Writing

$$B'_{ijk} = E^{-1}_{i\alpha}B_{\alpha\beta\gamma}E_{\beta j}E_{\gamma k} \quad (39)$$

we note that this is also periodic with the period of the original periodic orbit and can be developed as a Fourier series. Then, when the evaluation of the second-order terms is performed, Eq. (36) becomes

$$\frac{\mathrm{d}}{\mathrm{d}t}z = \mathcal{J}z + \boldsymbol{f}(t) \quad (40)$$

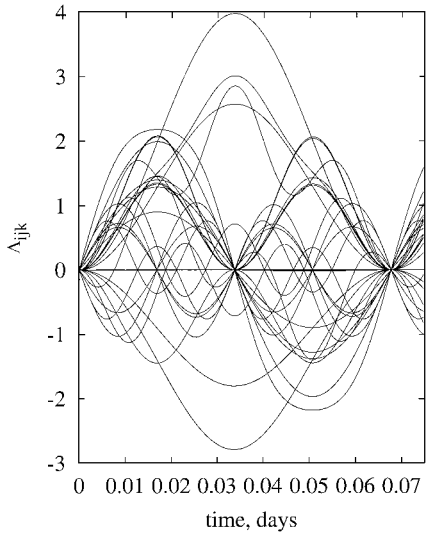

Fig. 5 Λ_{ijk} components over one orbit, showing only the part with no secular terms.

where the forcing term is

$$f_i(t) = \tfrac{1}{2!} B'_{i\alpha\beta} e^{\mathcal{J}\delta t}_{\alpha\gamma} e^{\mathcal{J}\delta t}_{\beta\delta} z_\gamma(t_0) z_\delta(t_0) \tag{41}$$

Then, the second-order free-oscillation solution can be written using standard linear system techniques as

$$z_i(t) = e^{\mathcal{J}\delta t}_{i\alpha} [z_\alpha(t_0) + \Lambda_{\alpha\beta\gamma}(t) z_\beta(t_0) z_\gamma(t_0)] \tag{42}$$

The first term in Eq. (42) is the zero-order solution (37), whereas the remainder represents the desired second-order perturbations. The second-order perturbations are given by the definite integral

$$\Lambda_{ijk}(t) = \frac{1}{2!} \int_{t_0}^{t} e^{-\mathcal{J}\delta t}_{i\alpha} B'_{\alpha\beta\gamma} e^{\mathcal{J}\delta t}_{\beta j} e^{\mathcal{J}\delta t}_{\gamma k} \, \mathrm{d}t \tag{43}$$

Closed-form evaluation of this integral is detailed in the Appendix.

Examining Eq. (43), and remembering that B' is periodic, we might expect secular terms (terms growing linearly in time) and mixed secular terms (terms involving both a periodic term and a term proportional to time) for those components of Λ_{ijk} involving a term in time in Eq. (38). Secular terms could also arise from a nonzero constant term in the B' Fourier series. The existence of further secular and mixed secular terms in the second-order solution is important because it governs whether more directions of instability appear, other than the two directions present in the first-order solution. Figure 5 shows the behavior of the Λ_{ijk} over slightly more than one orbit. Components of Λ_{ijk} for $i \neq 3, 5$ and $j, k \neq 4, 6$ have been suppressed. That is, we have excluded the two directions z_3 and z_5 already known to possess secular terms and excluded the two initial conditions $z_4(t_0)$ and $z_6(t_0)$ known to cause such secular terms. The resulting Fig. 5 shows that the remainder of Λ_{ijk} is periodic. This means that no new unstable behavior appears at the second order for zonal perturbations, other than that which appeared in the first-order solution.

However, this does not mean that if the modal variables $z_4 = 0$ and $z_6 = 0$ that the cluster will remain together. There are secular terms due to nonzero values of z_i, $i \neq 4, 6$, that produce, in particular, in-track dispersion of the cluster. These must be calculated to keep the cluster accurately together in one region of space.

Perturbations from Outside Forces

To construct a periodic orbit, some forces were excluded from the baseline dynamics. Although the inclusion of the zonal harmonics brings the important J_2 term into the reference solution, all sectoral and tesseral gravitational harmonics have been excluded, as well as air drag. There is a fairly simple way that their effects may be included in the solution, however. Because they have been excluded from the baseline dynamics and the Taylor's series expansion of the dynamics about the periodic orbit, they first appear in the nodal frame variational equations (29) or the modal variational equations (36) with lowest-order terms that are the force evaluated on the periodic orbit itself. The next-order terms will involve the differential effects of these forces across the span of the satellite cluster: the first-order terms in $\delta\mathcal{N}$ or z. These higher-order terms will involve, for example, the differential gravitational acceleration of a tesseral harmonic term across the diameter of the cluster, or the extra air drag experienced by an individual satellite because of its motion about the cluster center. The effects of these first-order perturbations will be extremely small compared to the already small effects of the zero-order terms.

Because both the nodal frame system (29) and the modal frame system (36) are linear systems, and because these extra forces, when evaluated on the periodic orbit, become functions of time alone, we obtain a linear system with a time-dependent forcing function. One simple way to incorporate these forces is to obtain the particular solution to the linear system by numerical integration. The nodal variable particular solution is the result of integrating

$$\frac{\mathrm{d}}{\mathrm{d}t}\mathcal{Y}_i = A_{i\alpha}\mathcal{Y}_\alpha + \mathcal{R}^{(2)}_Z \begin{Bmatrix} \mathbf{0} \\ \boldsymbol{a}_p \end{Bmatrix} \tag{44}$$

with $\mathcal{Y}_i = 0$ at the initial time. This form can be thought of as including the perturbations from outside forces in the description of the periodic orbit itself. Alternately (and, to this author, preferably), the modal frame particular solution is the result of numerically integrating

$$\frac{\mathrm{d}}{\mathrm{d}t} z_i = \mathcal{J}_{i\alpha} z_\alpha + E^{-1}(t) \mathcal{R}^{(2)}_Z \begin{Bmatrix} \mathbf{0} \\ \boldsymbol{a}_p \end{Bmatrix} \tag{45}$$

again with zero initial conditions $z_i = 0$ at the initial time. Of course, the purpose in calculating the particular solution is so that the effects of these perturbations can be subtracted to give the free oscillations. This means that the satellite's control system will not be burdened with maneuvers to null out possibly benign perturbations of the cluster as a whole.

Although we are numerically integrating Eq. (45) to obtain the forced perturbations, our method still holds a great advantage over a simple all-encompassing numerical integration of the equations of motion in, for example, the inertial frame. Such a numerical integration would not give the analyst any insight into which part of the integration produces effects that can be tolerated, for example, purely periodic effects, and which part of the integration will tear the cluster apart. A modern satellite theory must inevitably resort to numerical integration to handle the wide variety of forces that must be included in a state-of-the-art model. However, the current theory identifies and separates the acceptable and unacceptable effects to a very high order of accuracy.

One important modification can be made to these equations that greatly extends their range of validity. The periodic orbit and $E(t)$ matrix are represented by Fourier series, and it is a simple matter to insert an arbitrary phase angle in the evaluation of these series, $\omega_0 t \to \omega_0 t + \phi$, where $\omega_0 = 2\pi/\tau$ is the periodic orbit frequency. Now, a small change in this phase angle will cause a small displacement along the state-space velocity vector. However, this is redundant with the third Floquet mode z_3, which is also a displacement along the state-space velocity vector. Using a phase angle in the periodic orbit is a global description of this effect, whereas the Floquet mode z_3 is the equivalent local description. Because we expect significant in-track perturbations, especially due to air drag, we have elected to replace the local in-track mode z_3 with the global phase angle ϕ in the periodic orbit. The equivalent in-track displacements are

$$\dot{\boldsymbol{X}}_0 \delta t = \dot{\boldsymbol{X}}_0 \delta\phi/\omega_0 = \boldsymbol{f}_3 z_3 \tag{46}$$

From this we find

$$\phi = \omega_0 (|\boldsymbol{f}_3|/|\dot{\boldsymbol{X}}_0|) z_3 \tag{47}$$

using that $\boldsymbol{f}_3$ and $\dot{\boldsymbol{X}}_0$ are strictly collinear. Then, reducing this to a differential equation gives

$$\dot{\phi} = \omega_0(|\boldsymbol{f}_3|/|\dot{\boldsymbol{X}}_0|)\dot{z}_3 \tag{48}$$

which will completely replace the $\dot{z}_3$ equation of motion in Eq. (45). Because we are effectively declaring $z_3 \equiv 0$ for all time, there is no term in the preceding involving time derivatives of the vector magnitudes.

Numerical Results

In this section, we report on numerical results obtained by the methods given earlier. The reference periodic orbit used has an orbital altitude of 637 km and an inclination of 1 rad. We will include all zonal harmonics through order and degree 14 from the EGM96 model.[18] Of course, the zonal harmonics go into the periodic orbit solution, whereas the sectoral and tesseral harmonics are a source of perturbations.

Begin with the second-order perturbations due to the two-body and zonal harmonic terms. We have already seen that these terms do not introduce any additional sources of instability, other than those already present due to the two terms linear in time in the Floquet reference solution. Figure 6 shows the modal variables z_i over one orbit, where the displacements from the periodic orbit were chosen to be large enough that the second-order perturbation effects are visible. Over one orbit, the free oscillation in the eccentricity mode (z_1 and z_2) has too long a period to be visible, so that without second-order perturbations, all of these curves should be straight lines. The continuous curve was produced by numerically integrating the full trajectory and then solving for the osculating modal variables. The theoretical values from the methods discussed earlier are shown as points along each of the six curves. There is very accurate agreement at this level, which corresponds to about a 1-km eccentricity oscillation, combined with a 10-km separation in track. The two modes linear in time have here been excited at a level that will be unacceptable in an actual satellite cluster, to observe their second-order perturbations as well. This shows up as nonzero values of z_4, a change in the Keplerian period, and z_6, a change in the z angular momentum/nodal regression rate. Of course, these perturbations become larger (and less accurately modeled) as the separation from the periodic orbit increases. However, even for smaller-sized satellite clusters, accurate modeling of the second-order free oscillations will mean that they will not be responsible for unnecessary control usage.

In calculating the perturbations from other forces, we have included all sectoral and tesseral harmonics from the EGM96 model through order and degree 14. The acceleration due to air drag

$$\boldsymbol{a}_{\text{drag}} = -\tfrac{1}{2}B^*\rho v\boldsymbol{v} \tag{49}$$

was included in the inertial frame numerical integration, with a ballistic coefficient $B^* = 0.1$ m^2/kg. The atmospheric density ρ model was taken from Regan and Anandakrishran.[19] From here on, all

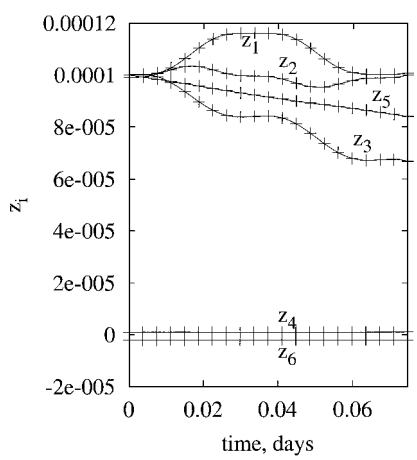

Fig. 6 Second-order zonal perturbations in the modal variables z_i over one orbit.

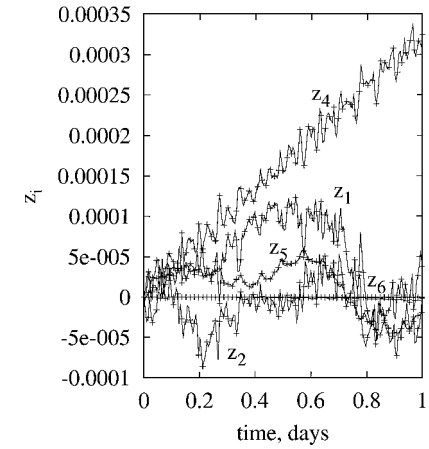

Fig. 7 Forced perturbations in the modal variables z_i.

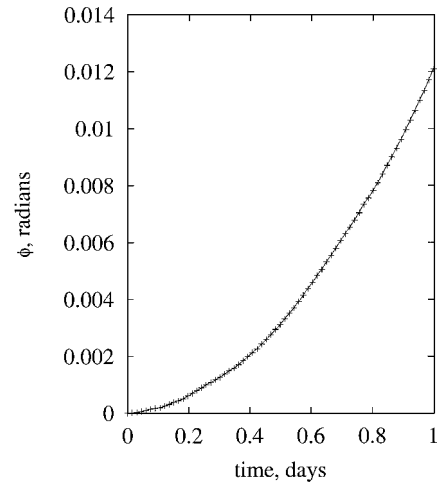

Fig. 8 Perturbations in the periodic orbit phase angle ϕ.

cases will have the initial values $z_4 = 0$ and $z_6 = 0$ to suppress any tendency of the solution to depart from the reference periodic orbit by virtue of the Floquet solution. Numerically integrated trajectories can be transformed from the inertial frame to the modal variables z_i for comparison with the particular solution. Alternately, the inertial coordinates can be calculated from the free and particular solution and compared with the inertial frame results.

Figure 7 shows the behavior of the modal variables z_i under the influence of sectoral and tesseral gravitational harmonics and air drag, with the exception of z_3. Instead of z_3, Fig. 8 shows the behavior of the periodic orbit phase variable ϕ. Both integrations cover a period of one day. Again, the solid curve comes from the numerical integration in inertial rectangular coordinates transformed to the modal variables. Points show the theoretical predictions from the numerical integration of the particular solution equations of motion (45). The effect of air drag is to produce a quadratic departure in the periodic orbit phase and to impart a linear drift to z_4, which is essentially the orbital energy. Use of the orbit phase ϕ extends the time until it becomes necessary to shift the reference periodic orbit to one that is more representative of the actual cluster orbit. Without air drag, the forced perturbations in all six modal variables are essentially periodic. Eventually the drift in z_4 will exceed the validity of the linearization, and a more representative periodic orbit must be chosen. The agreement between the inertial frame numerical integration and the modal variable forced perturbations is better than 1 m and is often at the centimeter level.

As a final numerical experiment, we combine both second-order and particular solutions in one single orbital calculation. Also, instead of showing plots of the modal variables, we plot the position error of the satellite, calculated as the magnitude of the difference between the inertial frame integrated position and the equivalent result from the modal variable perturbation work. Figure 9 shows

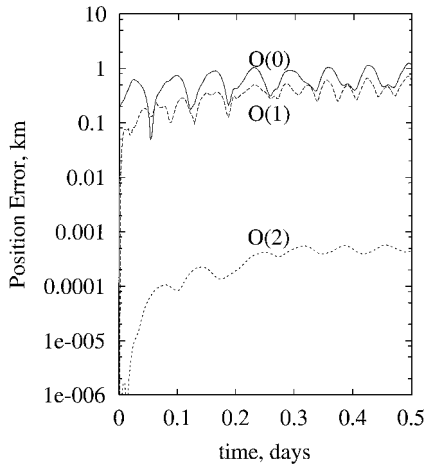

Fig. 9 Position prediction accuracy for one-half day, without air drag.

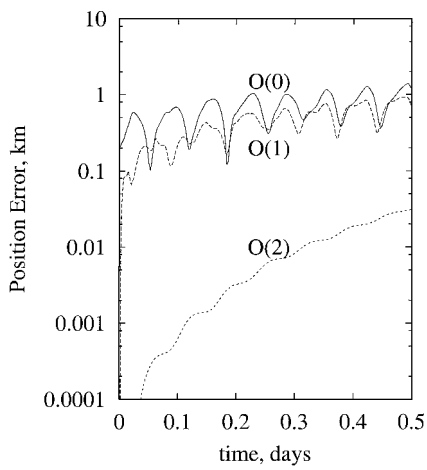

Fig. 10 Position prediction accuracy for one-half day, with air drag included.

the position prediction error for a cluster with a free-oscillation amplitude of about 1 km from the periodic orbit. In the case shown in Fig. 9, there is no air drag force on the satellites. The curve labeled $\mathcal{O}(0)$ is the raw periodic orbit itself, included so that the magnitude of the free oscillation about that orbit can be seen. (Of course, the periodic orbit uses the perturbed phase ϕ, so that it remains locked to the actual solution.) The Floquet solution without perturbations is shown in the curve labeled $\mathcal{O}(1)$. The Floquet solution in this case is not much of an improvement because the free-oscillation amplitude has been chosen to be very small. Finally, the curve labeled $\mathcal{O}(2)$ includes both the second-order free oscillations from zonal gravitational terms and the first-order forced solution from all sectoral and tesseral gravity harmonics through order and degree 14. This latter curve achieves a prediction error of better than 50 cm after one-half of a day.

Including air drag presents a considerably greater challenge. Figure 10 shows the same case as the preceding experiment but now with air drag included in the dynamic model. Again, individual curves show the position prediction error for the periodic orbit, the Floquet solution, and the predicted second-order perturbations. Position errors at the end of one-half day now rise to about 25 m. This is, of course, an open-loop experiment. An actual satellite cluster will use an estimation technique to fit both the periodic orbit, modal amplitudes z_i, and air drag B^* to actual data. It is suspected that this will significantly improve the accuracy.

With accurate modeling of the dynamics, it will not be necessary to waste stationkeeping fuel in an attempt to null benign natural perturbations. The control problem reduces to suppressing the two linear drift rates present in the Floquet solution: the differential Keplerian period drift excited by a nonzero value of the modal variable z_4 and the differential nodal regression excited by the modal variable z_6. Actually, the dynamic mismodeling itself will be a source of a waste of stationkeeping fuel. If we take the results of the last simulation at face value, an error of 100 m in one day can be canceled by a maneuver of 1.1 mm/s over one day. (This equates to less than 40-m/s Δv requirement in a five-year lifetime.)

Discussion

In this paper we have reported on a new relative motion solution for satellites that is, in a very real sense, an improved analogue of the CW solution. The current solution uses the two-body problem plus all zonal harmonics as its baseline dynamics, whereas the baseline dynamics of the CW solution is the two-body problem. The CW solution linearizes about a circular orbit and produces a set of constant coefficient linear equations, whereas the current method linearizes about a nearly circular periodic orbit and produces a set of time-periodic linear differential equations. The classic CW solution is solved with standard linear system techniques in the orbital frame of reference, and has one mode linear in time. The current solution is produced via Floquet theory, again in the same orbital frame of reference, and produces two modes linear in time. The second secular mode is associated with differential regression of the nodes for different values of the orbital Z angular momentum, as reported by Schaub and Alfriend.[2] The CW solution can be expressed as one circular orbit plus one time-dependent matrix, the state transition matrix. The current solution is completely described by one periodic vector, the periodic orbit $\mathcal{N}_0(t)$, and one periodic matrix function, the modal matrix $F(t)$. The current solution includes all of the familiar features of the classical CW solution, but, in addition, contains all of the zonal harmonics, especially the dominant oblateness term J_2.

Conclusions

The periodic orbit/linear Floquet solution to satellite relative motion discussed in the early part of this paper already includes many dynamic effects not present in the CW solution. However, all of the rest of the dynamics present in a fully realistic problem can be included in either a second-order free-oscillation solution driven by the two-body and zonal harmonics, or in a particular solution including all other dynamic effects. The second-order two-body/zonal harmonic solution was obtained analytically and does not introduce any additional sources of instability beyond that already present in the Floquet solution. Sectoral and tesseral gravitational harmonics and air drag have been modeled by constructing a particular solution to the time-periodic linear system. This has been done numerically. The particular solution can be extended by recognizing that one mode of the linear system, z_3, is the local expression of changing the global phase of the periodic orbit reference solution. Forces modeled in the particular solution to lowest order affect the dynamics of all satellites in the cluster equally. In effect, the particular solution is a perturbation of the periodic orbit itself. Perhaps most important, air drag will cause the cluster orbits to decay slowly, but to quite high accuracy will not separate the individual satellites, assuming that they all have the same ballistic coefficient.

The actual overall closed-loop stationkeeping requirements will need to include the actual control method, the navigation and orbit determination problem, any mismatch between the modeled and actual dynamics, and errors introduced by performing the maneuvers. With the ability to treat the dynamics accurately, we can proceed to design control systems in the linear, but time-periodic, system, once second-order and forced perturbations are subtracted.

Appendix: Second-Order Free Oscillations

The second-order terms in the zonal problem require the evaluation of the integral (43). We wish to perform this task analytically to see whether any further instabilities appear. The state transition matrix for the first-order solution is given by Eq. (38), and the tensor B'_{ijk} from Eq. (39) is available as a Fourier series. Counting up the possibilities from $\exp(\mathcal{J}\delta t)$, we can have terms involving $\cos\omega_1\delta t$, $\sin\omega_1\delta t$, and t, raised to powers up to three. There will also be contributions from the Fourier series representation of the B' tensor in sines and cosines of $\omega_0 t$, where ω_0 is the frequency of the periodic

orbit. Then, suppressing all i, j, and k dependence in Eq. (43), we must integrate objects of the form

$$\Lambda = \int_{t_0}^{t} \sum_{\alpha\beta\gamma}^{6} \sum_{\epsilon=0}^{\infty} \frac{1}{2}(\pm 1)\{c_\epsilon \cos\epsilon\omega_0 t + s_\epsilon \sin\epsilon\omega_0 t\} \times (\cos\omega_1 t)^{n_1}(\sin\omega_1 t)^{n_2} t^{n_3}\, \mathrm{d}t \tag{A1}$$

Here, c_ϵ and s_ϵ are Fourier series coefficients from a particular term of $B'_{\alpha\beta\gamma}$ and the integers n_1, n_2, and n_3 come from counting the occurrence of these terms in the particular term of the tensor product in Eq. (43), as does the factor ± 1.

Now, we replace the trigonometric functions with their complex exponential equivalents. The B' Fourier series term becomes

$$c_\epsilon \cos\epsilon\omega_0 t + s_\epsilon \sin\epsilon\omega_0 t = \mathcal{C} e^{i\epsilon\omega_0 t} + \mathcal{C}^* e^{-i\epsilon\omega_0 t} \tag{A2}$$

where $\mathcal{C} = (c_\epsilon - i s_\epsilon)/2$, and the asterisk denotes the complex conjugate. The standard identities are used to replace $\cos\omega_1 t$ and $\sin\omega_1 t$ with their complex equivalents. Then, using the binomial theorem twice gives

$$\Lambda = \sum_{\alpha\beta\gamma}^{6} \sum_{\epsilon=0}^{\infty} \left(\frac{1}{2}\right)^{1+n_1+n_2} (\pm 1)(-i)^{n_2} \sum_{\lambda=0}^{n_1} \sum_{\sigma=0}^{n_2} \frac{n_1!}{(n_1-\lambda)!\lambda!} \times \frac{n_2!(-1)^{n_2}}{(n_2-\sigma)!\sigma!} \int_{t_0}^{t} \{\mathcal{C} e^{\upsilon_1 t} t^{n_3} + \mathcal{C}^* e^{\upsilon_2 t} t^{n_3}\}\, \mathrm{d}t \tag{A3}$$

Here,

$$\upsilon_1 = i[\epsilon\omega_0 + (n_1 + n_2 - 2\lambda - 2\sigma)\omega_1]$$
$$\upsilon_2 = i[-\epsilon\omega_0 + (n_1 + n_2 - 2\lambda - 2\sigma)\omega_1] \tag{A4}$$

and $0! = 1$ when it occurs.

The actual integrations have now been reduced to elementary integrals. For completeness, we cite the necessary results

$$\int e^{\upsilon t}\, \mathrm{d}t = \frac{1}{\upsilon} e^{\upsilon t}, \qquad \int t e^{\upsilon t}\, \mathrm{d}t = \frac{\upsilon t - 1}{\upsilon^2} e^{\upsilon t}$$
$$\int t^2 e^{\upsilon t}\, \mathrm{d}t = \frac{\upsilon^2 t^2 - 2\upsilon t + 2}{\upsilon^3} e^{\upsilon t}$$
$$\int t^3 e^{\upsilon t}\, \mathrm{d}t = \frac{\upsilon^3 t^3 - 3\upsilon^2 t^2 + 6\upsilon t - 6}{\upsilon^4} e^{\upsilon t}$$

These integrals will be real valued, although they are most conveniently evaluated with complex arithmetic. Also, for $\epsilon = 0$, there are some values of the summations over λ and σ that lead to one or both of the $\upsilon_i = 0$. In this case, the integrals become the familiar

$$\int t^{n_3}\, \mathrm{d}t = \frac{1}{n_3 + 1} t^{n_3 + 1} \tag{A5}$$

It is the terms containing powers of time that are of concern in the free second-order solution, the secular and mixed secular terms. We have taken the trouble to construct this semi-analytical solution (using numerically determined Fourier coefficients for B') to the second-order perturbation problem to determine where such terms occur. In practice, it may be simpler to include the second-order two-body/zonal perturbations by direct numerical integration of Eq. (36) instead of Eq. (45).

Acknowledgments

This research was supported by the U.S. Air Force Research Laboratory and the State of Ohio through the Dayton Area Graduate Studies Institute, Grant VA-UC-99-01.

References

[1]Clohessy, W., and Wiltshire, R., "Terminal Guidance Systems for Satellite Rendezvous," *Journal of the Aerospace Sciences*, Vol. 27, No. 9, 1960, pp. 653–658.

[2]Schaub, H., and Alfriend, K., "J_2 Invariant Relative Orbits for Spacecraft Formations," NASA CP-1999-209235, 1999.

[3]Sedwick, R., Miller, D., and Kong, E., "Mitigation of Differential Perturbations in Clusters of Formation Flying Satellites," *Journal of the Astronautical Sciences*, Vol. 47, No. 4, 2000, pp. 309–331.

[4]Melton, R., "Time-Explicit Representation of Relative Motion Between Elliptical Orbits," *Journal of Guidance, Control, and Dynamics*, Vol. 23, No. 4, 2000, pp. 604–610.

[5]Carter, T. E., "State Transition Matrices for Terminal Rendezvous Studies: Brief Survey and New Example," *Journal of Guidance, Control, and Dynamics*, Vol. 21, No. 1, 1998, pp. 148–154.

[6]Gim, D., and Alfriend, K., "The State Transition Matrix of Relative Motion for the Perturbed Non-Circular Reference Orbit," American Astronautical Society, AAS Paper 01-222, 2001.

[7]Ulybyshev, Y., "Long-Term Formation Keeping of Satellite Constellation Using Linear Quadratic Controller," *Journal of Guidance, Control, and Dynamics*, Vol. 21, No. 1, 1998, pp. 109–115.

[8]de Queiroz, M., Kapila, V., and Yan, Q., "Adaptive Nonlinear Control of Multiple Spacecraft Formation Flying," *Journal of Guidance, Control, and Dynamics*, Vol. 23, No. 3, 2000, pp. 385–390.

[9]Sparks, A., "Satellite Formationkeeping Control in the Presence of Gravity Perturbations," *Proceedings of the American Control Conference*, American Automatic Control Council, Evanston, IL, 2000, pp. 844–848.

[10]Floquet, M. G., "Équations Différentielles Linéaires à Coefficients Périodiques," *Annales Ecolé Normale Superior*, Vol. 12, Ser. 2, 1883, pp. 47–88.

[11]Nickerson, K., Herder, R., Glass, A. B., and Cooley, J. L., "Application of Altitude Control Techniques for Low Altitude Earth Satellites," *Journal of the Astronautical Sciences*, Vol. 26, No. 2, 1978, pp. 129–148.

[12]Rosborough, G., and Ocampo, C. A., "Influence of Higher Degree Zonals on the Frozen Orbit Geometry," *Advances in the Astronautical Sciences*, Vol. 76, Pt. 2, 1991, pp. 1291–1304.

[13]Shapiro, B. E., "Phase Plane Analysis and Observed Frozen Orbit for the Topex/Poseidon Mission," *Advances in the Astronautical Sciences*, Vol. 91, 1995, pp. 853–872.

[14]Brouwer, D., and Clemence, G., *Methods of Celestial Mechanics*, Academic Press, New York, 1961, pp. 108–113.

[15]Wiesel, W. E., "Perturbation Theory in the Vicinity of a Periodic Orbit," *Celestial Mechanics*, Vol. 23, No. 3, 1981, pp. 231–242.

[16]Wiesel, W. E., and Pohlen, D. J., "Canonical Floquet Theory," *Celestial Mechanics and Dynamical Astronomy*, Vol. 58, No. 1, 1994, pp. 81–96.

[17]Calico, R. A., and Wiesel, W. E., "Control of Time-Periodic Systems," *Journal of Guidance, Control, and Dynamics*, Vol. 7, No. 6, 1984, pp. 671–676.

[18]Pavlis, N., Kenyon, S., and Manning, D., "Gravity Anomaly Data," URL: http://www.cddisa.gsfc.nasa.gov/926/egm96/egm96.html, 1996.

[19]Regan, F., and Anandakrishran, S., *Dynamics of Atmospheric Reentry*, AIAA, Washington, DC, 1993, pp. 537–540.